

Three-dimensional measurements on the mandible of patients with hemifacial microsomia

Meng Wang, Lai Gui

Department of Craniomaxillofacial Surgery, Plastic Surgery Hospital, Chinese Academy of Medical Sciences, Peking Union Medical College, Beijing 100144, China.

Abstract

Background: Hemifacial microsomia (HFM), which involves multiple sites with different levels of severity, is the second most common congenital craniofacial deformity after cleft lip and palate. However, three-dimensional (3D) measurements of mandibular deformities have not yet been studied in detail. The objective of this study is to investigate the method of 3D measurements of mandibular deformities in HFM patients.

Methods: A total of 48 HFM patients were included in this study. All clinical treatment for patients was performed in the Plastic Surgery Hospital of the Chinese Academy of Medical Sciences at Peking Union Medical College from June 2006 to June 2020. The patients' 3D computerized tomography scan data were processed using medical imaging software, following four iterative steps: 3D reconstruction, mirroring, differential analysis, and partition.

Results: The characteristics of the mandibular bone in HFM patients are mainly presented as follows: (1) compared to the normal side, the part of the bone body that extends from the ascending ramus to the pogonion (Po-NB) is analyzed using a dynamic process: less fullness-fullness-more fullness; (2) absences were frequently observed among the angular zones, that is, the height of the ascending ramus is deficient.

Conclusions: HFM is a complicated condition with numerous variations in clinical presentation. We employed both 3D image reconstruction and computerization image processing techniques to investigate asymmetrical mandibular deformity in HFM patients in detail and with great accuracy. This will be of great use to clinicians for disease management.

Keywords: Hemifacial microsomia; Mandibular deformity; Three-dimensional measurement

Introduction

Hemifacial microsomia (HFM) is the second most common congenital craniofacial deformity, after cleft lip and palate. Besides, it involves multiple sites with different levels of severity. Mandibular dysplasia (known as MDP syndrome) is the most frequent and complex skeletal deformity associated with HFM.^[1,2] The clinical features of MDP syndrome mainly present dysplasia or the loss of bone in the ascending ramus of the mandibular bone. Also, various presentations are found among patients with MDP in the ascending ramus, such as flatness of the articular surface of the condyle, dysplasia, or abnormal position of the temporomandibular joint, temporomandibular joint absence at the base of the skull, or an enlarged angle of the mandible.^[3-5]

To achieve the optimal treatment outcome, it is essential to conduct a thorough pre-operative evaluation and surgical plan before elective surgery for HFM patients. However, conventional approaches are mainly based on two-

dimensional measurements from skull X-rays,^[6,7] which makes it challenging to capture the characteristics of the deformity and obtain a comprehensive understanding of the individual case. To assist surgical planning, we conducted an exploratory experiment using three-dimensional (3D) measurements of the mandibular bone for 48 HFM patients.

Methods

Ethical Approval

Ethics approval for this study was approved by the Medical Ethics Committee at the Plastic Surgery Hospital (PSH) (No. 2022-6). Informed consent was obtained from all individual participants involved in the study.

Study Population

A total of 48 HFM patients were included in this study: 27 females (56.3%) and 21 males (43.8%). Twenty-three patients were presented with left-sided HFM, while the remaining cases had right-sided HFM. The mean age of the

Access this article online

Quick Response Code:



Website:
www.cmj.org

DOI:
10.1097/CM9.0000000000002116

Correspondence to: Meng Wang, Department of Craniomaxillofacial Surgery, Plastic Surgery Hospital, Chinese Academy of Medical Sciences, Peking Union Medical College, Beijing 100144, China
E-Mail: s2006131@163.com

Copyright © 2022 The Chinese Medical Association, produced by Wolters Kluwer, Inc. under the CC-BY-NC-ND license. This is an open access article distributed under the terms of the Creative Commons Attribution-Non Commercial-No Derivatives License 4.0 (CCBY-NC-ND), where it is permissible to download and share the work provided it is properly cited. The work cannot be changed in any way or used commercially without permission from the journal.

Chinese Medical Journal 2022;135(8)

Received: 26-06-2021; Online: 15-04-2022 Edited by: Ningning Wang

study population was 19 years, ranging from 13 to 27 years. All clinical procedures were performed in the PSH of the Chinese Academy of Medical Sciences at Peking Union Medical College between June 2006 and June 2020.

Image Analysis Methods

The patients’ 3D computerized tomography (CT) scan images were processed according to four iterative steps using medical image software: 3D reconstruction, mirroring, differential analysis, and partition.

3D Reconstruction

Primary 3D CT scan data in the Digital Imaging and Communications in Medicine format were used as the input in the medical imaging software (Brilliance 64, Philips, Netherlands) for further processing. Individualized threshold values were applied for hard-tissue reconstruction of the skull, and a 3D image of the skull was subsequently generated.

Mirroring

The mirror plane was determined using three points on the reconstructed 3D skull image [shown in Figure 1]: the nasal root point, the intersection point of the sagittal seam and the herringbone seam, and the intersection point between the foramen magnum and the external occipital ridge. The image of the deformed side was then replaced with a mirror image of the normal side to attain a symmetrical 3D image.

Differential Analysis

Next, differential analysis was performed on the overlapping images between the mirrored 3D image and the original image under the same coordinates. Two different software applications were employed to process the 3D images: Imageware v12.0 and Geomagic Studio v9.0. The former was used for pre-processing, while the latter was used to label the differences between the pre- and postmirror images, using pre-defined colors.

Partition

The overlapping 3D images were adjusted into a standardized measurement plane of the skull lateral view. Adjusted images were then partitioned into six zones after referencing clinical observations. First, horizontal and vertical lines were generated from the distal tooth cervix on the surface of the mandibular second molar. Next, vertical lines were drawn from the intersection point between the ramus of the mandible and the body of the mandible on the occlusal surface of the mandibular second molar. Finally, two individual vertical lines were drawn from the mental foramen on the mirrored pane. Ultimately, the patient’s mandibular image was partitioned into six zones: a, b, c, d, e, and f, as Figure 2A illustrates. Zone a represents the upper half area of the mandibular ramus, b and c signify the lower H area of the mandibular ramus, d denotes the mandibular body area, e is the chin area, and f represents the mandibular angle. Differential analysis was conducted within the individual zones. Measurements were quantified using default coordinates of the CT scans and were recorded at up to four digits after the decimal place. A paired *t* test was conducted to compare the mean differences between the same measurements of two phases for the same patients. Differences measured between normal and deformed sides were semi-quantitative, as follows: “+” denotes that the deformed side is more convex than the normal side with a difference <5 mm at the apex; “++” indicates that such a difference is between 5 and 10 mm; “-” means that the deformed side is more concave than the normal side with a difference <5 mm at the bottom; “--” shows that the difference is in the range of 5 to 10 mm.

Results

Table 1 presents the results of the semi-quantitative analysis of the mandibular bone images between the deformed side and the normal side of the 48 patients. The comparison was made individually in Zones A–E after standardization. The proportion of HFM patients who presented convex deformed sides was 2%, 19%, 83%,

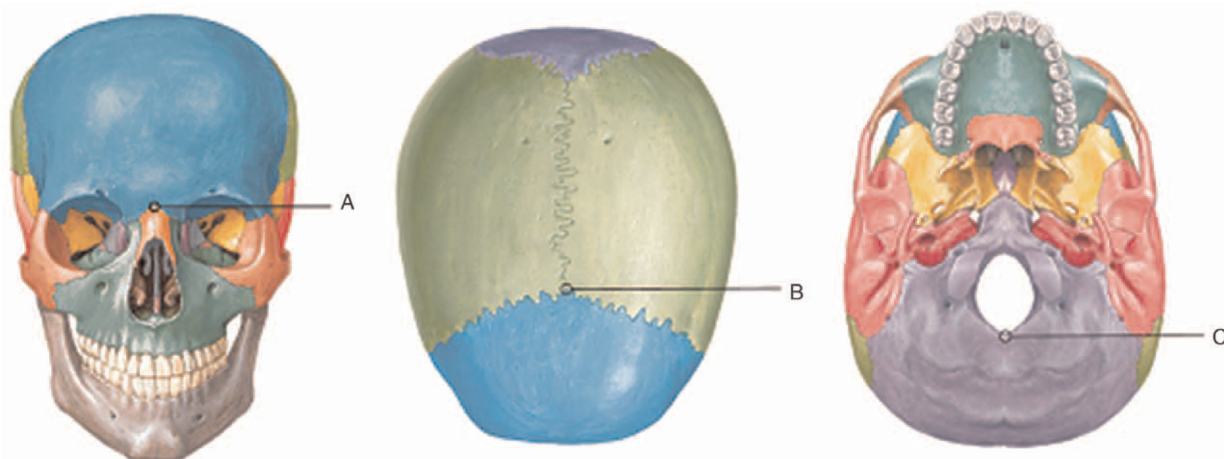


Figure 1: Determine the mirror plane using three points: (A) nasal root point; (B) intersection point of the sagittal seam and the herringbone seam; (C) intersection point between the foramen magnum and the external occipital ridge.

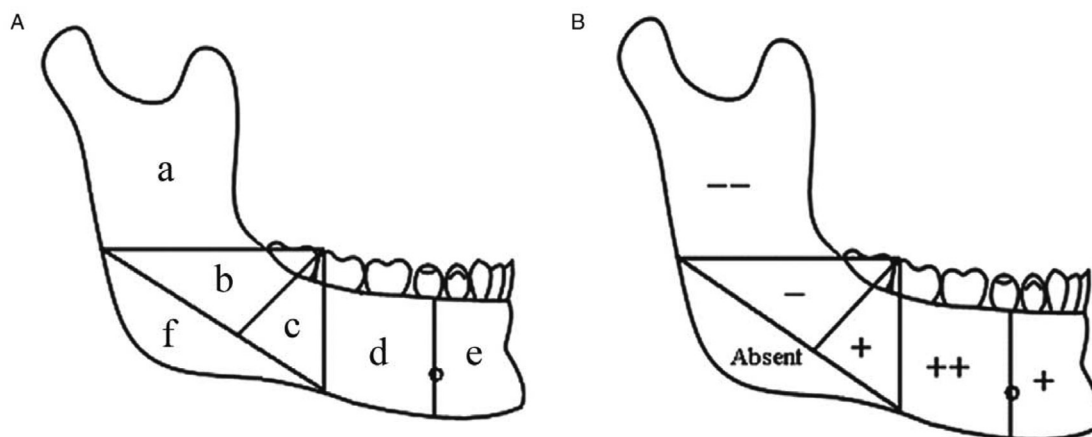


Figure 2: (A) Illustration of the mandibular partition; Zone a represents the upper half area of the mandibular ramus, b and c signify the lower 1/2 zarea of the mandibular ramus, d denotes the mandibular body area, e is the chin area, and f represents the mandibular angle. (B) Mandibular bone characteristics of HFM patients. HFM: Hemifacial microsomia. “+” denotes that the deformed side is more convex than the normal side with a difference <5 mm at the apex; “++” indicates that such a difference is between 5 and 10 mm; “-” means that the deformed side is more concave than the normal side with a difference <5 mm at the bottom; “--” shows that the difference is in the range of 5 to 10 mm.

Table 1: Comparison of the mandibular bone image between the deformed side and the normal side within Zones A-E after standardization.

Items	Zone				
	A	B	C	D	E
Convex deformed side (count)	1	9	40	46	47
Convex deformed side (%)	2	19	83	96	98
Average difference between deformed side and healthy side	--	-	+	++	+

“+” denotes that the deformed side is more convex than the normal side with a difference <5 mm at the apex; “++” indicates that such a difference is between 5 and 10 mm; “-” means that the deformed side is more concave than the normal side with a difference <5 mm at the bottom; “--” shows that the difference is in the range of 5 to 10 mm.

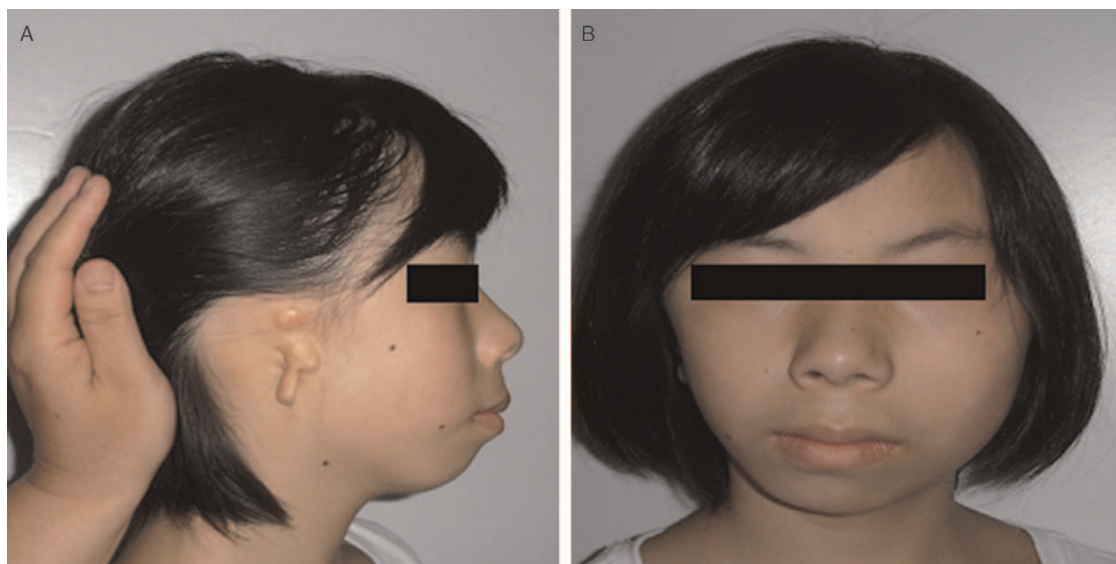


Figure 3: Typical case: a 14-year-old female with HFM on the right side. (A) Lateral, (B) front. HFM: Hemifacial microsomia.

96%, and 98%, respectively. A comparison of Zone F shows that 88% of patients presented a complete absence of bone in this region, while 54% of patients showed a reduced width of the lower face.

The characteristics of the mandibular bone of HFM patients are mainly presented as follows: (1) compared to

the normal side, a part of the bone body from the ascending ramus to the pogonion (Po-NB) was examined utilizing a dynamic process: less fullness-fullness-more fullness; (2) absences were frequently observed among angular zones, that is, the height of the ascending ramus was reduced. Figure 2B presents a visual representation of our findings Figure 3.

Typical case: A typical case is a 14-year-old female who was diagnosed with congenital right-sided HFM. After 3D image reconstruction, mirroring, differential analysis, and partition, the patient displayed a lack of

height in the ascending ramus [shown in Figure 4]. However, the absence of the deformed side did not result in a reduction in the width of the lower part of the face.

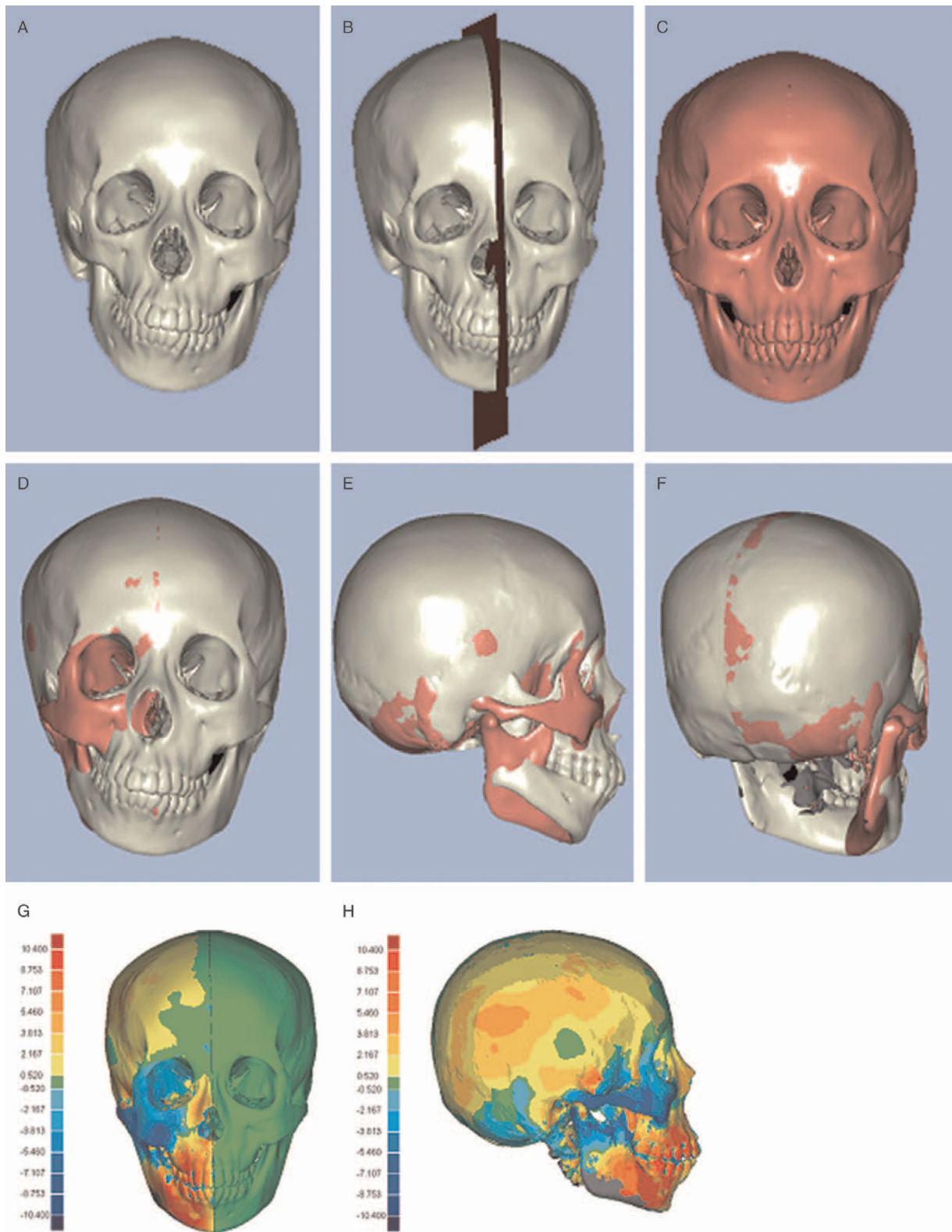


Figure 4: (A–C) The mirroring process: (A) before mirroring; (B) mirror plane; (C) after mirroring; (D–F) differential analysis with Imageware v12.0. The white part is the original three-dimensional skull image of the patient, and the pink part is the mirror image; (G–H) differential analysis with Geomagic Studio v9.0. The difference between the images before and after mirroring is presented: (G) frontal view; (H) lateral view. Value range: -10.4 to 10.4 mm.

Discussion

Significance of 3D Measurements

HFM is also known as craniofacial microsomia, first and second branchial arch syndrome, or lateral facial dysplasia. As the second most common congenital facial deformity after cleft lip and palate, the crude incidence rate is about 1/3500 to 1/5600 of total live births.^[3] This malformation involves multiple anatomic locations and various levels of severity.^[8] The most frequent and also the most complicated bone deformity among this group of patients is a mandibular deformity. Therefore, the treatment for mandibular deformity is the foundation of the clinical management of HFM.^[9,10] Current treatments include lengthener implantation, osteotomy, and augmentation, with the primary objective being symmetrical facial structure and deformity correction.^[11,12] A detailed and comprehensive understanding of the deformity contributes to an individualized surgical plan and eventually leads to better treatment outcomes.^[13,14] However, conventional measurement of HFM is generally based on 2D skull X-ray images, which may not be sufficient to capture a complete picture of the characteristics of each individual deformity. Evidence from research suggests that 3D measurements can achieve preciseness up to 0.01 mm. The mean difference of distance between 3D measurements and the conventional 2D approach is about 5.64 mm, and the average difference of the angular distance is approximately 3.69°. Compared to direct measurements of skull specimens, 3D imaging has demonstrated excellent accuracy, with an average difference of 0.19 mm. Evidence from this study demonstrates that 3D CT scans could be used as an accurate and valid tool for facial cranial research studies.^[15,16]

Choice of Reference Points

It is crucial to establish reference points on the skull surface for the 3D imaging technique. Apart from a few mild cases, most HFM patients present extensive asymmetrical deformities including asymmetries in the mandibular, maxillary, zygomatic, or orbital regions. Severe cases, such as asymmetrical pathological changes, may even affect the temporal bone.

Due to the unique facial cranial pathological characteristics of HFM patients, conventional reference points such as Po-NB, superior alveolar base (SNA), and inferior alveolar base (ANB) may not apply in HFM cases. In this study, we chose reference points that were located far from each other and adopted ones where the extent of the deformity was mild: the nasion, the intersection point between the occipital foramen and the external occipital protuberance (referred to as the “anonymous point” in this study), and the intersection point between the sagittal suture and the lambdoid suture (the “lambdoid point”). These three points were employed to establish a plane for conducting the mirror procedure. During the case analysis, we discovered that this mirror plane did not fit one patient who had severe asymmetry of the skull. Therefore, this case was excluded from the final analysis.

Stability of Reference Points

To ensure the validity and replicability of the results of this study, we performed repeated calibration procedures to test the stability of the reference points in two phases with a 2-week interval. Given that the stability of the nasion has been widely studied, we did not replicate the test on this point, and the test was only performed for the anonymous point and lambdoid point. During the first phase, six repeated measurements were conducted on the 3D reconstructed skull images by a cranial facial surgeon within 1 week. The values of these two reference points on the 3D coordinate system were labeled as X, Y, and Z. The same procedure as Phase 1 was repeated 2 weeks later in Phase 2. A paired *t* test was performed using SPSS v13.0 software, and results show that the anonymous point and lambdoid point both have good stability ($P > 0.05$).

Results of 3D Measurements

As Table 1 shows, only one case presented fullness in Zone A with a significant difference observed between the deformed side and the normal side. In Zone D, 96% of patients displayed a convex deformed shape, and the average difference between the two sides was significant. A possible explanation for this could be that the MDP of the deformed side results in the uneven development of the mandible. Besides, the position of the condyle of both sides is relatively stable. Therefore, increased resistance in the ascending ramus of the mandible on the deformed side affects the development of the ascending ramus. This also results in a shift of the Po-NB to the normal side. Consequently, during surgical treatment, clinical discretion should be made based on the individual patient's needs, and augmentation to an underdeveloped area on the deformed side or an osteotomy for the convex normal side should be offered.

The majority of the patients (88%) presented an absence in Zone F, which is caused by dysplasia. Dysplasia of the ascending ramus of the mandible can result in a decrease in the height of the ascending ramus, with 54% of patients presenting reduced face width. Therefore, height reduction of the ascending ramus is a feature of HFM patients. However, surgical procedures to increase facial width should be offered according to the individual patient's clinical presentation.

Conclusions

In this study, both 3D image reconstruction and computerized image processing techniques were employed to investigate in detail asymmetrical mandibular deformity in HFM patients. Results from this study demonstrate a regular trend regarding the morphological presentation of the mandibular structure among patients. This will assist clinicians in the treatment of HFM patients.

We established that HFM is a complicated condition with large variations in clinical presentation, thus there is no agreed standardized procedure for surgical treatment based on current medical evidence. To date, this is the

comprehensive study that includes the deformity of bone tissue without the consideration of the possible asymmetrical deformity in cartilage tissue. Besides, the mirror plane adopted for making measurements in this study is a relatively straight forward reference. However, clinicians should be cautious when applying the results of this study in clinical practice and should consider the medical needs of individual patients.

Funding

This work was supported by a grant by Key Clinical Program of the Ministry of Health (No. 2010-132).

Conflicts of interests

None.

References

1. Grabb WC. The first and second brachial arch syndromes. *Plast Reconstr Surg* 1965;36:485–508. doi:10.1097/00006534-196511000-00001.
2. Yamaguchi K, Lonc D, Ko EWC, Lo LJ. An integrated surgical protocol for adult patients with hemifacial microsomia: methods and outcome. *PLoS One* 2017;12:e0177223. doi: 10.1371/journal.pone.0177223.
3. Gorlin RJ. Deformations and disruptions. *Syndromes of the Head and Neck*. 3rd ed. New York: Oxford University Press; 1990.
4. Steinbacher DM, Gougoutas A, Bartlett SP. An analysis of mandibular volume in hemifacial microsomia. *Plast Reconstr Surg* 2011;127:2407–2412. doi: 10.1097/PRS.0b013e3182131cc8.
5. Bertin H, Mercier J, Cohen A, Giordanetto J, Cohen N, Lee SH, *et al*. Surgical correction of mandibular hypoplasia in hemifacial microsomia: a retrospective study in 39 patients. *J Craniomaxillofac Surg* 2017;45:1031–1038. doi: 10.1016/j.jcms.2017.03.016.
6. Tokura TA, Miyazaki A, Igarashi T, Dehari H, Kobayashi JL, Miki Y, *et al*. Quantitative evaluation of cephalometric radiographs of patients with hemifacial microsomia. *Cleft Palate Craniofac J* 2019;56:711–719. doi: 10.1177/1055665618813453.
7. Fattah AY, Caro C, Khechayan DY, Tompson B, Forrest CR, Phillips JH. Cephalometric outcomes of orthognathic surgery in hemifacial microsomia. *J Craniofac Surg* 2014;25:1734–1739. doi: 10.1097/SCS.0000435808.91512.58.
8. Wang J, Liu E, Du L, Hu M. Soft tissue damage in patients with hemifacial microsomia. *J Craniofac Surg* 2019;30:2449–2450. doi: 10.1097/SCS.0000000000005824.
9. Birgfeld C, Heike C. Craniofacial microsomia. *Clin Plast Surg* 2019;46:207–221. doi: 10.1016/j.cps.2018.12.001.
10. Young A, Spinner A. *Hemifacial Microsomia*. Treasure Island, FL: StatPearls Publishing; 2020.
11. Taiwo AO. Classification and management of hemifacial microsomia: a literature review. *Ann Ib Postgrad Med* 2020;18:S9–S15.
12. Heike CL, Hing AV, Aspinall CA, Bartlett SP, Birgfeld CB, Drake AF, *et al*. Clinical care in craniofacial microsomia: a review of current management recommendations and opportunities to advance research. *Am J Med Genet C Semin Med Genet* 2013;163C:271–282. doi: 10.1002/ajmg.c.31373.
13. Xu X, Zhang ZY, Li BH, Tang XJ, Yin L, Liu W. Three-dimensional measurement of maxillary involvement in hemifacial microsomia in children. *J Craniofac Surg* 2020;31:444–447. doi: 10.1097/SCS.00000000000006200.
14. Dumas BM, Nava A, Law HZ, Smartt J, Derderian C, Seaward JR, *et al*. Three-dimensional printing for craniofacial surgery: a single institution's 5-year experience. *Cleft Palate Craniofac J* 2019;56:729–734. doi: 10.1177/1055665618798292.
15. Ko EWC, Chen PK, Lo LJ. Comparison of the adult three-dimensional craniofacial features of patients with unilateral craniofacial microsomia with and without early mandible distraction. *Int J Oral Maxillofac Surg* 2017;46:811–818. doi: 10.1016/j.ijom.2017.03.002.
16. Anderson PJ, Yong R, Surman TL, Rajion ZA, Ranjitkar S. Application of three-dimensional computed tomography in craniofacial clinical practice and research. *Aust Dent J* 2014;59:174–185. doi: 10.1111/adj.12154.

How to cite this article: Wang M, Gui L. Three-dimensional measurements on the mandible of patients with hemifacial microsomia. *Chin Med J* 2022;135:971–976. doi: 10.1097/CM9.0000000000002116